Optimizing the electrode size and arrangement in a microbial electrolysis cell

Gil-Carrera, L.; Mehta, P.; Escapa, A.; Moran, A.; Garcia, V.; Guiot, S. R.; Tartakovsky, B.

Publisher's version / Version de l'éditeur:
https://doi.org/10.1016/j.biortech.2011.08.026
Bioresource Technology, 102, 20, pp. 9593-9598, 2011-08-10

Bioresource Technology 102 (2011) 9593–9598

Contents lists available at SciVerse ScienceDirect

Bioresource Technology

journal homepage: www.elsevier.com/locate/biortech

Optimizing the electrode size and arrangement in a microbial electrolysis cell

L. Gil-Carrera [a,b], P. Mehta [b], A. Escapa [a], A. Morán [a], V. García [c], S.R. Guiot [b], B. Tartakovsky [b,*]

[a] Chemical Engineering Department, University of León, IRENA-ESTIA, Avda. de Portugal 41, León 24009, Spain
[b] Biotechnology Research Institute, National Research Council of Canada, 6100 Royalmount Ave, Montreal, QC, Canada H2P 2R2
[c] Isolux-Corsan S.A., C/Caballero Andante 8, 28021 Madrid, Spain

ARTICLE INFO

Article history:
Received 10 June 2011
Received in revised form 2 August 2011
Accepted 4 August 2011
Available online 10 August 2011

Keywords:
MEC
Hydrogen
Gas diffusion cathode
3D anode

ABSTRACT

This study investigates the influence of anode and cathode size and arrangement on hydrogen production in a membrane-less flat-plate microbial electrolysis cell (MEC). Protein measurements were used to evaluate microbial density in the carbon felt anode. The protein concentration was observed to significantly decrease with the increase in distance from the anode–cathode interface. Cathode placement on both sides of the carbon felt anode was found to increase the current, but also led to increased losses of hydrogen to hydrogenotrophic activity leading to methane production. Overall, the best performance was obtained in the flat-plate MEC with a two-layer 10 mm thick carbon felt anode and a single gas-diffusion cathode sandwiched between the anode and the hydrogen collection compartments.

1. Introduction

Microbial electrolysis cells (MECs) are bioelectrochemical reactors producing hydrogen through microbially catalyzed electrolysis of organic matter (Logan et al., 2008). Since this process was first reported (Liu et al., 2005b; Rozendal et al., 2006), the MEC design has been constantly improving resulting in a substantial increase of the volumetric efficiency (Rozendal et al., 2008). However, the application of the MEC technology to wastewater treatment requires further research to improve the design and develop inexpensive electrode materials with a high specific surface area, good conductivity, and a high stability. Several anode materials have been recently tested in MECs, including graphite granules, reticulate vitreous carbon, carbon foam, and graphite brush electrodes (Aelterman et al., 2006; Chaudhuri and Lovley, 2003; He et al., 2005; Logan et al., 2007; Zuo et al., 2007). The benefits of three dimensional (3D) anodes, which provide increased surface area for microbial attachment (Aelterman et al., 2008; Logan et al., 2007; Zhang et al., 2011), have been demonstrated by comparing a packed bed of irregular graphite granules with three different thicknesses to a one-dimensional configuration (Di Lorenzo et al., 2010). Also, higher power outputs were observed in microbial fuel cells (MFCs) that have a 3D anode architecture (Chen et al., in press; Kim et al., 2011; Logan et al., 2007). However, the carbon source and proton transport limitations might limit the acceptable anode thickness (Sleutels et al., 2009; Torres et al., 2008), thus necessitating a more detailed study.

The cathode surface area is also crucial in optimizing MEC performance. The hydrogen evolution reaction often limits the overall MEC performance and cathodes with a larger surface area have demonstrated an increase in hydrogen production and current density (Call et al., 2009). Also, both MFC and MEC tests have demonstrated that the maximum power output can be increased by reducing the distance between the electrodes (Ghangrekar and Shinde, 2007; Liu et al., 2005a; Zhang et al., 2009).

The study presented below evaluates the influence of the anode and cathode size and configuration on the volumetric efficiency of hydrogen production in a flat-plate membraneless MEC with a gas diffusion cathode and demonstrates that by optimizing the anode–cathode configuration the hydrogen production could be substantially increased.

2. Methods

2.1. Analytical methods and MEC characterization

Acetate was analyzed in an Agilent 6890 gas chromatograph (Wilmington, DE) equipped with a flame ionization detector. Gas flow was measured by bubble counters interfaced with a data acquisition system (Tartakovsky et al., 2009). The MEC current was recorded every 20 min using a data acquisition board (Labjack Corp, Lakewood, CO, USA). The gas composition was measured using a gas chromatograph (6890 Series, Agilent Technologies, Wilmington, DE) equipped with a 11 m × 3.2 mm 60/80 mesh Chromosorb 102 column (Supelco, Bellefonte, PA, USA) and a thermo conductivity detector. The carrier gas was argon. The pH and conductivity of the effluent were measured using a pH meter

* Corresponding author. Tel.: +1 514 496 2664; fax: +1 514 496 6265.
E-mail address: Boris.Tartakovsky@nrc-cnrc.gc.ca (B. Tartakovsky).

0960-8524/$ - see front matter Crown Copyright © 2011 Published by Elsevier Ltd. All rights reserved.
doi:10.1016/j.biortech.2011.08.026

(Accumet Excel XL 30, Fisher Scientific, Pittsburgh, PA) and a conductivity meter (Accumet Basic AB 15, Fisher Scientific, Pittsburgh, PA), respectively. Additional details are provided in Tartakovsky et al. (2009).

MEC voltage scans were performed by changing the applied voltage between 0.4 V and 1.3 V with a step of 0.2 V and 10 min intervals at each voltage setting to allow for current stabilization. Internal resistance (R_{int}) was calculated using voltage scan results as the slope of the linear portion of the voltage vs current curve. More details are provided in Manuel et al. (2010).

The MEC performance was characterized using current and hydrogen production measurements at a steady state. Also, the Coulombic efficiency (E_{coul}), cathodic efficiency (E_{cath}), and energy consumption (apparent and equivalent) were calculated. The apparent energy consumption was calculated based on the measured H_2 production. The equivalent energy consumption considered CH_4 production from H_2, in addition to the H_2 produced (Manuel et al., 2010). To account for anode size (volume) differences in each test, the current density was expressed per carbon felt volume (mA L_A^{-1}). To provide a basis for comparison with other works, the hydrogen production was expressed per anode compartment (i.e. reactor) volume (L_{H2} L_R^{-1} d^{-1}).

2.2. Protein quantification

Protein quantification was performed to determine the relative amount of microorganisms in the anodic biofilm. Carbon felt samples, 1 cm × 1 cm × 0.5 cm were taken from the middle and bottom of each anode, cut with scissors into pieces, and were put into sterile 2 mL tubes with 500 mg of 0.1 and 0.5 mm sterile glass beads (zirconia/silica beads, Biospec Products, Inc., Bartlesville, OK, USA). Tubes were then filled with sterile distilled water, vortexed to mix the beads and anode pieces and bead-beaten for 15 s twice using FastPrep® system (Bio 101 Savant, Bio/Can Scientific, Mississauga, ON, Canada) at a speed setting of 5.5. Subsequently, the samples were centrifuged and the supernatant collected and concentrated in a DNA concentrator (Savant DNA120 SpeedVac® concentrator, Thermo Fisher Scientific, Asheville, NC, USA). The samples were then analyzed following the Bio-Rad protein assay protocol (Bio-Rad Laboratories Ltd., Mississauga, ON, Canada).

2.3. Ni-cathode preparation

The nickel solution was prepared using 150 mM $NiSO_4{\cdot}6H_2O$, 25 mM $NiCl_2{\cdot}6H_2O$, 500 mM H_3BO_3 and 1 CTAB cetyl trimethylammonium bromide, and heated to 55 °C. An air pump was installed to ensure mixing so that the Ni was uniformly distributed in the solution during its deposition on the cathode. A Ni-foam was attached to one side of the container and on the opposite side the carbon paper (Sigracet GDL 25 BC, SGL Group, Germany) for the cathode was attached (Manuel et al., 2010).

A power supply (2400 SourceMeter, Keithley, Cleveland, OH, USA) was connected to the cathode (negative pole) and the Ni-foam (positive pole) and a current of 100 mA for 10 min was applied. Subsequently, to eliminate the unattached Ni particles, the cathode was soaked and rinsed in distilled water 4 times and then sonicated for 20 s. The cathode was then dried in the oven at 95–100 °C for 2 h. The cathode was weighed using the analytical balance before and after electrodeposition to measure the amount of Ni electrodeposited.

2.4. MEC construction and operation

Two continuous flow MECs, MEC-1 and MEC-2, were constructed with a series of nylon plates. MEC 1 had a 50 mL anodic compartment and MEC 2 had a 100 mL anodic compartment. The hydrogen collection (cathodic) compartments had a volume of 50 mL each and were attached to one or both sides of the anodic compartment. The anodic compartments contained 1–4 layers of 5-mm thick GFA-5 carbon felt measuring 10 × 5 cm (SGL Group, Kitchener, ON, Canada). Each piece of carbon felt had an estimated volume of 25 mL. Titanium rods with an Ir-MMO coating (Magneto Special Anodes B.V., The Netherlands) were inserted into the felt and used as current collectors. Gas diffusion cathodes, prepared as described above, were separated from the anodes using a polyester cloth with a thickness of approximately 0.7 mm and sandwiched between the anode compartment and the H_2 collection compartment.

The MECs were inoculated with 5 mL of a homogenized anaerobic mesophilic sludge obtained from a local food processing industry (A. Lassonde Inc., Rougemont, QC, Canada) and operated at 30 °C. A solution of carbon source and nutrients was continuously fed using an infusion pump (model PHD 2000, Harvard Apparatus, Canada) at 5.0 mL d^{-1}. The carbon source stock solution contained (in g L^{-1}): sodium acetate (55.2), yeast extract (0.8), NH_4Cl (18.7), KCl (148), K_2HPO_4 (64), and KH_2PO_4 (40.6). The dilution water contained 1 mL of a trace metals (TM) stock solution prepared according to Tartakovsky et al. (2008). The carbon source solution was fed at a rate of 5–10 mL d^{-1} with a syringe pump. Dilution water with TM was fed at a rate of 226 mL d^{-1}. In the separate test aimed at inhibiting methane production, 2-bromoethanesulfonate (BES) was added to the dilution water (42.2 g-BES L^{-1}). The carbon source and dilution water streams were combined before entering the anodic compartment. The resulting influent stream had a conductivity of 12–14 mS cm^{-1}. An external recirculation loop was used for anodic liquid mixing. The liquid was taken at the compartment top and returned through the influent port at a rate of 0.29 L/h.

For the sake of comparison, the MECs were operated at an applied voltage of 1 V throughout all tests. The applied voltage was controlled using an adjustable power source (2400 SourceMeter, Keithley, Cleveland, OH, USA). All tested anode–cathode configurations were maintained for a minimum period of 72 h to insure a steady state. The MEC was considered to be in steady state when the hydrogen production rate and the current generation was stable (i.e. no trends were observable within a period of 48 h).

MEC-1 and MEC-2 were initially started using a one anode and one cathode configuration (1A–1C). Then MEC-1 was modified by adding an additional anode (2A–1C configuration) and then an additional cathode was added (2A–2C configuration). At the end of MEC-1 tests, it was modified to contain a single compartment without a H_2-collection compartment. MEC-2 was also modified during the test to contain four anodes (4A–1C configuration) and then a second cathode was added (4A–2C). All tested MEC configurations are listed in Table 1. Also, 1A–1C and 4A–2C configurations are illustrated in Fig. 1.

3. Results and discussion

3.1. The effect of anode thickness on hydrogen production

The tests were started with MEC-1 and MEC-2 being operated in a 1A–1C configuration. Once MEC-1 reached a steady state, the average current was 31.9 mA. Based on the carbon felt volume of 25 mL, a corresponding current density of 1.28 mA L_A^{-1} was estimated. Also, the hydrogen production was 211 mL d^{-1} (8.44 L L_A^{-1} d^{-1}). The results obtained for MEC-2 were slightly different with a lower current of 23.7 mA (0.74 mA L_A^{-1}). These current measurements were used as a basis for comparison with the other configurations.

After observing a steady-state performance, MEC-1 was modified by adding an additional piece of carbon felt to test the

Table 1
MEC performance as a function of MEC configuration (number of carbon felt layers and cathodes). Cathodic efficiency was calculated based on H_2 flow.

MEC number/ configuration	Anode compartment (mL)	Carbon felt volume (mL)	Current (mA)	H_2 flow (mL d^{-1})	H_2 and CH_4 flow in H_2 eq (mL d^{-1})	E_{coul} (%)	E_{cath} (%)
MEC-1 1A/1C	50	25	31.9 ± 3	210	245.6	69.1	65.5
MEC-1 2A/1C	50	50	41.7 ± 10.4	242	295.8	66.5	57.5
MEC-1 1A/2C	50	25	38.1 ± 1.9	83	144.2	67.1	20.6
MEC-1 2A/2C	50	50	54.5 ± 7.6	178	199.7	96.8	30.6
MEC-2 4A/1C	100	100	28.1 ± 4.5	272	372.6	76.7	64.9
MEC-2 4A/2C	100	100	49.8 ± 7.7	258	294.3	86.6	49.8
MEC-2 4A/2C (BES)	100	100	30.1 ± 4.5	157	181.9	59.8	49.0
MEC-1 one compartment	50	25	25.5 ± 3.3	78	82.3	59.21	35.1

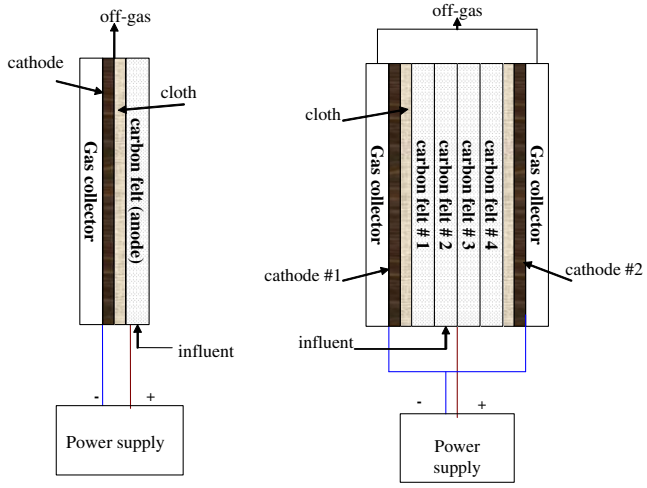

Fig. 1. Design of single anode–single cathode (1A–1C) and multi-anode–multi cathode (4A–2C) MECs.

2A–1C configuration. At a steady state, this configuration resulted in an increase in current to 41.7 mA (0.83 mA L_A^{-1}). Hydrogen production also increased and reached 245 mL d^{-1}, which was higher than in the 1A–1C configuration. More details are provided in Fig. 2A and B.

The influence of carbon felt anode thickness (i.e. anode volume) on MEC performance was further investigated by installing four new carbon felts in MEC-2 to obtain a total anode thickness of about 2 cm while using one cathode (4A–1C configuration). As in the MEC-1 test, the increased anode volume resulted in a higher current of 28.10 mA and a gas production of 272 mL d^{-1}. Despite the current increase, both MEC-1 with two carbon felts and MEC-2 with four carbon felts had a similar performance in terms of H_2 production, that is by increasing the number of carbon felt layers from 2 to 4 the MEC performance was not increased. Furthermore, the four carbon felt anodes increased the anode volume to 100 mL, leading to a lower volumetric current density of 0.29 mA L_A^{-1} (Fig. 2A). Internal resistance estimation based on the voltage scans showed that the number of carbon felts did not affect the internal resistance, which remained in a range of 15–17 Ω. Also, apparent energy consumption for H_2 production was 3.5–4.5 Wh L^{-1}.

After observing a stable MEC-2 performance with four carbon felts, on day 16 of the 4A–1C test samples were taken from each carbon felt layer for protein analysis. The distribution of proteins in the MEC-2 anode is shown in Fig. 3A. The protein concentration was the highest in the anode adjacent to the cathode, while it was close to zero in the two furthest anodes. Assuming that the protein concentration is proportional to anodic biofilm density, it can be inferred that the highest biofilm growth occurred in the proximity to the cathode, with no significant growth in the two carbon felts farthest from the cathode. This conclusion agrees with the comparison of 4A–1C and 2A–1C configurations in terms of current density and H_2 production.

Interestingly, both in 4A–1C and 4A–2C configurations, the difference in protein concentrations was more pronounced in the samples taken from the center of the anode, i.e. about 5 cm from the feeding line entry located at the MEC bottom. The samples collected near the feed line entry to the anodic compartment showed some increase in the protein concentration even in the carbon felts located at a greater distance from the cathode, although the highest increase in protein density was again observed in the carbon felt adjacent to the cathode (Fig. 3A). There was, perhaps, a gradient of acetate distribution in the anodic compartment, where a higher level of acetate at the MEC bottom promoted growth of not only the exoelectricigenic microorganisms but also of the methanogens. It could be hypothesized that further from the acetate entry point (MEC middle) mostly the exoelectricigenic microorganisms proliferated in the cathode vicinity due to their higher

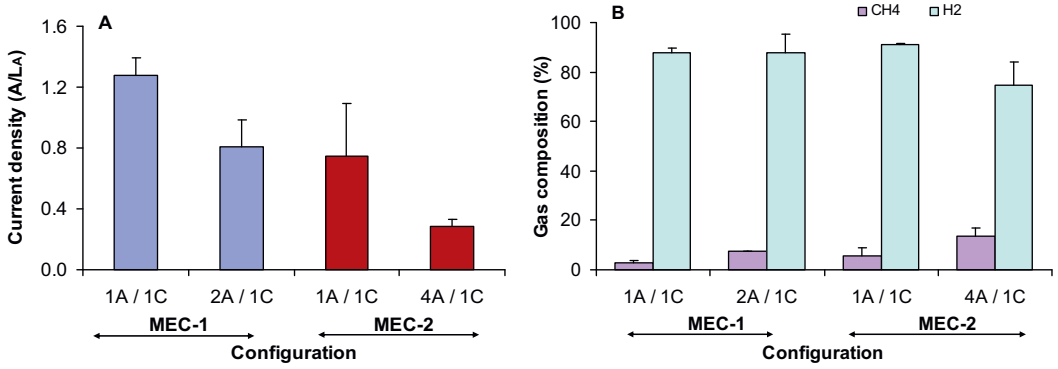

Fig. 2. Current density (A) and gas composition (B) observed in MECs with different anode thicknesses (one anode, two anodes, and four anodes) and a single cathode. The current density was calculated based on the anode volume.

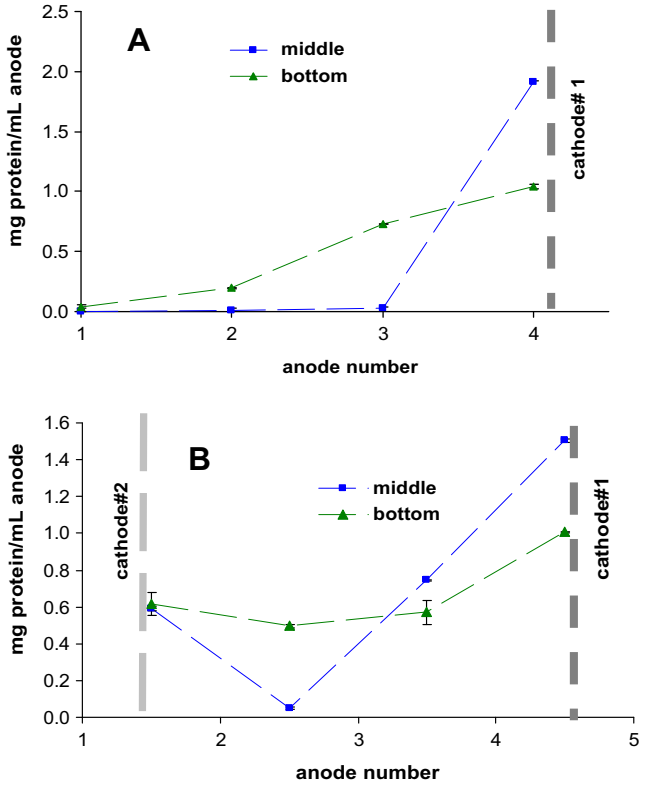

Fig. 3. Protein distribution observed in MEC-2 operated in (A) 4A–1C and (B) 4A–2C configurations. Anode samples were taken from the middle and bottom of the carbon felt measuring 10 cm × 5 cm.

affinity to acetate (Pinto et al., 2010). Overall, the exoelectricigenic microorganisms outcompeted the methanogens in the first anode layer, while the methanogens were likely present in the proximity to the carbon source entry line and in the following anode layers.

An obvious way of increasing current density would be to provide a greater anode surface area suitable for colonization by the exoelectricigenic microorganisms. Indeed, measured current and hydrogen production were increased when the number of carbon felt anodes was increased from one to two and then to four. However, the current increase was not directly proportional to anode thickness resulting in decreasing current density, which was estimated based on anode volume (Fig. 2 and Table 1). Although a higher volumetric current density was observed with a 5 mm anode, only 50% of the reactor volume was used. Considering that a multi-compartment design might increase construction costs, the anode thickness of 10 mm (two carbon felts) was considered an acceptable compromise for the given MEC design and operating conditions, e.g. flat-plate acetate-fed MEC with one cathode. It might be noted that the current could also be limited by the cathodic, rather than the anodic reaction. Also, such factors as anodic liquid conductivity, carbon source strength and composition, and MEC design might influence the choice of the anode size. In particular, MEC operation on wastewater might require the steps of carbon source hydrolysis and fermentation (Logan, 2004). To provide a support for hydrolytic and fermentative microorganisms the anode size could be increased or an additional (non-conductive) support for microbial growth could be provided. Alternatively, a pretreatment (acidification) step could be used for enhanced hydrolysis and fermentation of slowly degradable organic matter.

The results presented above also agree with the known dependence of MEC/MFC performance on the anode surface area and the distance between the electrodes. While 3D anodes improve MFC performance due to increased active surface area for biofilm growth, it was demonstrated that increasing the distance between cathode and anode decreases the MEC efficiency (Ghangrekar and Shinde, 2007; Liu et al., 2005a). This dependence is related to an increased resistance to proton transport with increasing distance (Gil et al., 2003). Consequently, the transport of protons released in carbon felt layers placed further from the cathode might limit the growth of exoelectricigenic microorganisms. A confirmation of proton transport limitation could be obtained by measuring pH values at different distances from the cathode (Vroom et al., 1999). Overall, we concluded that in order to maximize volumetric efficiency, relatively thin 3D anodes (e.g. 5–10 mm) with a large surface area for microbial attachment and good porosity to facilitate carbon source transport through the anode matrix should be used.

3.2. The effect of cathode configuration on hydrogen production

Once the 1A–1C and 2A–1C tests in MEC-1 were completed, the effect of the cathode configuration and surface area on MEC performance was studied. MEC-1 was modified to include two cathodes and two H_2-collection compartments (one on each side of the anode, Fig. 1) while maintaining a single carbon felt (1A–2C configuration). We immediately observed a higher current of 38.1 mA (1.52 mA L_A^{-1}) as compared to the 1A–1C design (Fig. 4A). However, the off-gas flow decreased and the flow contained less H_2 and more CH_4 (Fig. 4B). Nevertheless, when total gas production was estimated in terms of H_2 equivalent flow (where CH_4 was converted to its H_2 equivalent using reaction stoichiometry), the gas flow was directly proportional to current.

Following the 1A–2C test, the two cathodes–two anodes (2A–2C) configuration was also tested in MEC-1 by the addition

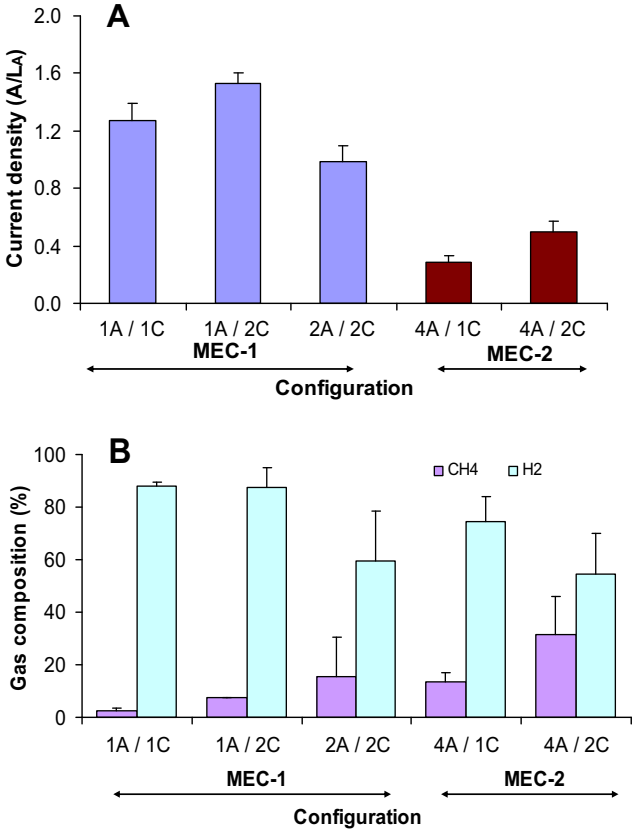

Fig. 4. Current density (A) and methane and hydrogen percentage (B) in the off-gas of MEC-1 and MEC-2 operated with different cathode configurations.

of the second carbon felt to the anodic compartment. This test showed an even higher current of 54.5 mA, but the current density slightly declined because of the increased anode volume (0.99 mA L_A^{-1}). However, a very low hydrogen production (178 mL d^{-1}) was obtained with this configuration because the methane percentage was further increased reaching 15.3%. Once again, total gas production expressed in the H_2 equivalent was directly proportional to current, i.e. both H_2 and CH_4 production was likely related to exoelectricigenic activity.

A similar pattern was observed in MEC-2 with four carbon felts when a second cathode was installed (4A–2C configuration). As in the test described above, the installation of the second cathode almost doubled the current up to 50 mA (0.50 mA L_A^{-1}). Once again, current density expressed per anode volume was less than in MEC-1 because of a significantly larger anode volume, 100 mL vs 25 mL (Table 1). H_2 production increased to 258 mL d^{-1} immediately after the second cathode was added, but then it decreased to levels comparable to those with one cathode. With time, the current remained unchanged while methane production increased thus leading to a decrease in cathodic efficiency calculated based on H_2 flow, as can be seen from the results provided in Table 1. The gas composition analysis (Fig. 4B) showed significant methane production (54.6% H_2 and 31.4% CH_4). Internal resistance estimation based on the voltage scan data in MEC-1 showed that the internal resistance decreased to 11–13 Ω. In single-cathode configurations (1A–1C and 2A–1C) a resistance of 15–17 Ω was estimated. Significant CH_4 production in the two-cathode tests led to high apparent energy consumption, up to 5.5 Wh L^{-1}. However, when the equivalent energy consumption and the cathodic efficiency were recalculated using the H_2 equivalent of the CH_4 produced, these parameters were estimated at 2–4 Wh L^{-1} and 50–70%, respectively.

After observing a stable MEC-2 performance in terms of gas production and composition, carbon felt anode samples were taken (17 d after second cathode installation) to study the protein distribution in the 4A–2C configuration. The results shown in Fig. 3B indicate a higher microbial population density relative to the one cathode configuration, and once again, the highest protein density was obtained for the carbon felt anodes adjacent to the cathodes. Also, the protein distribution gradient was less pronounced for the samples taken at the MEC bottom, which agrees with the protein distribution profiles obtained for 4A–1C configuration. The protein density of the carbon felt layer #4 adjacent to the second (newly installed) cathode was lower than the protein density in layer #1 (Fig. 3B) suggesting that although H_2 production and current were stable, the steady state distribution of the biofilm was not reached.

In addition to the tests described above, a single compartment MEC configuration was tested by replacing the H_2 collection compartment of MEC-1 with a solid plate so that both electrodes were installed in the same compartment and gas was collected in its headspace. This design featured a very low gas production (78 mL d^{-1}) with high CH_4 composition, although the current, as shown in Table 1, was comparable to the 1A–1C configuration. This suggests that although a single compartment design is useful for COD removal from wastewater, it is quite inefficient for H_2 production because of hydrogen availability to hydrogenotrophic methanogens. Apparently, without a H_2 collection compartment, the H_2 formed at the cathode surface was dissolved in the anodic liquid and was either consumed by the hydrogenotrophic methanogens or diffused towards the anode resulting in H_2 recycling. The hydrogenotrophic activity could be also inferred from the absence of CO_2 in the off-gas, although CO_2 formation by the exoelectricigenic microorganisms might be expected. Considering that CH_4 formation from H_2 requires CO_2, the absence of CO_2 in the off-gas is consistent with the hydrogenotrophic activity.

Overall, it appeared that CH_4 production from cathodic H_2 due to the hydrogenotrophic activity was the main cause of the low cathodic efficiency at certain MEC configurations. This pathway would explain the decrease in H_2 percentage and the increase in CH_4 percentage. However, CH_4 could be also produced by a microbiological process of acetate consumption by acetoclastic methanogens. Also, CH_4 could be produced by an electrochemical reaction at the cathode (Cheng et al., 2009).

To elucidate the preferred pathway of CH_4 formation in MEC-1 and MEC-2 the power supply was switched off for 3 d to test if CH_4 can be produced by acetoclastic methanogens from acetate. Very low CH_4 production was observed and acetate concentration in the effluent considerably increased. It was concluded that the acetoclastic activity did not play a major role in CH_4 formation.

The role of hydrogenotrophic methanogens in CH_4 production was confirmed by inhibiting their activity. The addition of BES to MEC-2 influent resulted in a significant decrease in methane percentage and an increased hydrogen percentage, i.e. the BES addition suppressed the hydrogenotrophic activity. However, at this concentration BES was also toxic for exoelectricigenic bacteria, since a significant decrease in gas production and current were observed with time (0.30 mA L_A^{-1} and 157 mL d^{-1}) as can be seen in Table 1.

Since methane production from acetate through acetoclastic methanogenic activity was excluded in the power supply shut-off test described above and electromethanogenesis was reported to require more negative cathode potentials (Cheng et al., 2009) than used in our tests (−1100 to −1200 mV vs an Ag/AgCl reference electrode (Hrapovic et al., 2010)), we concluded that most of methane production in MECs should be attributed to hydrogenotrophic methanogens. Similar results were obtained in other studies (Wang et al., 2009). The tests, however, did not explain the observed increase in CH_4 production in the two cathode MEC configurations (1A–2C, 2A–2C, and 4A–2C). We can only hypothesize that either H_2 diffusion through the porous cathode was reduced, or the hydrogenotrophic methanogens proliferated, which allowed a greater part of hydrogen to be consumed. Notably, the increase in CH_4 production coincided with increased cathode area, i.e. it could be hypothesized that by increasing cathode surface area an additional support for the formation of hydrogenotrophic biofilm in the vicinity of H_2 source was provided.

4. Conclusions

By operating MECs with several layers of carbon felt anode we demonstrated that the current and hydrogen production can be increased by employing a 3D anode. However, there is an optimal anode thickness. We also found that although the two-cathode configuration increases current and net gas production expressed in H_2 equivalent (e.g. H_2 and CH_4), this configuration also leads to increased hydrogenotrophic activity. Overall, in order to achieve high volumetric efficiency, a stackable MEC design should be used where gas diffusion cathodes are sandwiched between the anode and gas-collection compartments and relatively thin 3D anodes are employed.

Acknowledgements

Funding for this study was provided by Isolux-Corsan S.A., Spain and by Ministerio de Ciencia e Innovación (Reference No. ENE2009-10395). Assistance of Guido Santoyo in MEC set-up is greatly appreciated. NRC publication No. 50023.

References

Aelterman, P., Rabaey, K., Pham, H.T., Boon, N., Verstraete, W., 2006. Continuous electricity generation at high voltages and currents using stacked microbial fuel cells. Environ. Sci. Technol. 40, 3388–3394.

Aelterman, P., Versichele, M., Marzorati, M., Boon, N., Verstraete, W., 2008. Loading rate and external resistance control the electricity generation of microbial fuel cells with different three-dimensional anodes. Bioresour. Technol. 99, 8895–8902.

Call, D.F., Merrill, M.D., Logan, B., 2009. High surface area stainless steel brushes as cathodes in microbial electrolysis cells. Environ. Sci. Technol. 43, 2179–2183.

Chaudhuri, S.K., Lovley, D.R., 2003. Electricity generation by direct oxidation of glucose in mediatorless microbial fuel cells. Nature Biotechnol. 21, 1229–1232.

Chen, S.C., He, G., Carmona-Martinez, A.A., Agarwal, S., Greiner, A., Hou, H., Schroder, U., in press. Electrospun carbon fiber mat with layered architecture for anode in microbial fuel cells. Electrochemistry.

Cheng, S., Xing, D., Logan, B., 2009. Direct biological conversion of electrical current into methane by electromethanogenesis. Environ. Sci. Technol. 43, 3953–3958.

Di Lorenzo, M., Scott, K., Curtis, T.P., Head, I.M., 2010. Effect of increasing anode surface area on the performance of a single chamber microbial fuel cell. Chem. Eng. 156, 40–48.

Ghangrekar, M.M., Shinde, V.B., 2007. Performance of membrane-less microbial fuel cell treating wastewater and effect of electrode distance and area on electricity production. Bioresour. Technol. 98 (15), 2879–2885.

Gil, G.-G., Chang, I.-S., Kim, B.H., Kim, M., Jang, J.-K., Park, H.S., Kim, H.J., 2003. Operational parameters affecting the performance of a mediator-less microbial fuel cell. Biosens. Bioelectron. 18, 327–334.

He, Z., Minteer, S.D., Angenent, L.T., 2005. Electricity generation from artificial wastewater using an upflow microbial fuel cell. Environ. Sci. Technol. 39, 5262–5267.

Hrapovic, S., Manuel, M.F., Luong, J.H.T., Guiot, S.R., Tartakovsky, B., 2010. Electrodeposition of nickel particles on a gas diffusion cathode for hydrogen production in a microbial electrolysis cell. Int. J. Hydrogen Energy 35, 7313–7320.

Kim, M.H., Iwuchukwu, I.J., Shin, D., Sanseverino, J., Frymier, P., 2011. An analysis of the performance of an anaerobic dual anode-chambered microbial fuel cell. J. Power Sources 196, 1909–1914.

Liu, H., Cheng, S., Logan, B., 2005a. Power generation in fed-batch microbial fuel cells as a function of ionic strength, temperature, and reactor configuration. Environ. Sci. Technol. 39, 5488–5493.

Liu, H., Grot, S., Logan, B.E., 2005b. Electrochemically assisted microbial production of hydrogen from acetate. Environ. Sci. Technol. 39 (11), 4317–4320.

Logan, B., 2004. Extracting hydrogen and electricity from renewable resources. Environ. Sci. Technol. 38, 160A–167A.

Logan, B., Call, D., Cheng, S., Hamelers, H.V.M., Sleutels, T.H.J.A., Jeremiasse, A.W., Rozendal, R.A., 2008. Microbial electrolysis cells for high yield hydrogen gas production from organic matter. Environ. Sci. Technol. 42, 8630–8640.

Logan, B., Cheng, S., Watson, V., Estadt, G., 2007. Graphite fiber brush anodes for increased power production in air–cathode microbial fuel cells. Environ. Sci. Technol. 41, 3341–3346.

Manuel, M.-F., Neburchilov, V., Wang, H., Guiot, S.R., Tartakovsky, B., 2010. Hydrogen production in a microbial electrolysis cell with nickel-based gas diffusion cathodes. J. Power Sources 195, 5514–5519.

Pinto, R.P., Srinivasan, B., Manuel, M.-F., Tartakovsky, B., 2010. A two-population bio-electrochemical model of a microbial fuel cell. Bioresour. Technol. 101, 5256–5265.

Rozendal, R.A., Hamelers, H.V.M., Euverink, G.J.W., Metz, S.J., Buisman, C.J.N., 2006. Principle and perspectives of hydrogen production through biocatalyzed electrolysis. Int. J. Hydrogen Energy 31, 1632–1640.

Rozendal, R.A., Hamelers, H.V.M., Rabaey, K., Keller, J., Buisman, C.J.N., 2008. Towards practical implementation of bioelectrochemical wastewater treatment. Trends Biotechnol. 26, 450–459.

Sleutels, T.H.J.A., Lodder, R., Hamelers, H.V.M., Buisman, C.J.N., 2009. Improved performance of porous bio-anodes in microbial electrolysis cells by enhancing mass and charge transport. Int. J. Hydrogen Energy 34, 9655–9661.

Tartakovsky, B., Manuel, M.F., Neburchilov, V., Wang, H., Guiot, S.R., 2008. Biocatalyzed hydrogen production in a continuous flow microbial fuel cell with a gas phase cathode. J. Power Sources 182, 291–297.

Tartakovsky, B., Manuel, M.F., Wang, H., Guiot, S.R., 2009. High rate membrane-less microbial electrolysis cell for continuous hydrogen production. Int. J. Hydrogen Energy 34 (2), 672–677.

Torres, C.I., Marcus, A.K., Rittmann, B.E., 2008. Proton transport inside the biofilm limits electrical current generation by anode-respiring bacteria. Biotechnol. Bioeng. 100, 872–881.

Vroom, J.M., De Grauw, K.J., Gerritsen, H.C., Bradshaw, D.J., Marsh, P.D., Watson, G.K., Birmingham, J.J., Allison, C., 1999. Depth penetration and detection of pH gradients in biofilms by two-photon excitation microscopy. Appl. Environ. Microbiol. 65, 3502–3511.

Wang, A., Liu, W., Cheng, S., Xing, D., Zhou, J., Logan, B.E., 2009. Source of methane and methods to control its formation in single chamber microbial electrolysis cells. Int. J. Hydrogen Energy 34, 3653–3658.

Zhang, X., Cheng, S., Wang, X., Huang, X., Logan, B., 2009. Separator characteristics for increasing performance of microbial fuel cells. Environ. Sci. Technol. 43, 8456–8461.

Zhang, Y., Sun, J., Hou, B., Hu, Y., 2011. Performance improvement of air–cathode single-chamber microbial fuel cell using a mesoporous carbon modified anode. J. Power Sources 196, 7458–7464.

Zuo, Y., Cheng, S., Call, D., Logan, B.E., 2007. Tubular membrane cathodes for scalable power generation in microbial fuel cells. Environ. Sci. Technol. 41, 3347–3353.